European Journal of Medicinal Chemistry 171 (2019) 116–128

Contents lists available at ScienceDirect

European Journal of Medicinal Chemistry

journal homepage: http://www.elsevier.com/locate/ejmech

Research paper

N, N′, N″-trisubstituted guanidines: Synthesis, characterization and evaluation of their leishmanicidal activity

Rafael Dias do Espírito Santo [a, b, 1], Ángela María Arenas Velásquez [c, 1], Luana Vitorino Gushiken Passianoto [a, b], Alex Arbey Lopera Sepulveda [c], Leandro da Costa Clementino [c], Renata Pires Assis [c], Amanda Martins Baviera [c], Predrag Kalaba [d], Fábio Neves dos Santos [e], Marcos Nogueira Éberlin [e], Gil Valdo José da Silva [f], Martin Zehl [g], Gert Lubec [h], Márcia Aparecida Silva Graminha [c, **], Eduardo René Pérez González [a, b, *]

[a] *Laboratório de Química Orgânica Fina, Departamento de Química e Biologia, Faculdade de Ciências e Tecnologia, Universidade Estadual Paulista – UNESP, Campus de Presidente Prudente, Rua Roberto Simonsen, 305, 19060-900, Presidente Prudente, SP, Brazil*
[b] *Programa de Pós-Graduação em Ciência e Tecnologia de Materiais (POSMAT), Universidade Estadual Paulista – UNESP, São Paulo, Brazil*
[c] *Departamento de Análises Clínicas, Faculdade de Ciências Farmacêuticas, Universidade Estadual Paulista – UNESP, Campus de Araraquara, Rodovia Araraquara-Jaú, km1, 14800-903, Araraquara, SP, Brazil*
[d] *Department of Pharmaceutical Chemistry, Faculty of Life Sciences, University of Vienna, Althanstraße 14, 1090, Vienna, Austria*
[e] *Laboratório ThoMSon de Espectrometria de Massas, Instituto de Química, Universidade de Campinas – UNICAMP, Campinas, 13083-970, SP, Brazil*
[f] *Departamento de Química, Faculdade de Filosofia, Ciências e Letras de Ribeirão Preto, Universidade de São Paulo – USP, Avenida dos Bandeirantes, 3900, 14040-901, Ribeirão Preto, SP, Brazil*
[g] *Department of Analytical Chemistry, Faculty of Chemistry, University of Vienna, Währinger Straße 38, 1090, Vienna, Austria*
[h] *Department of Neuroproteomics, Paracelsus Medical University, Salzburg, Austria*

ARTICLE INFO

Article history:
Received 12 February 2019
Received in revised form
13 March 2019
Accepted 14 March 2019
Available online 21 March 2019

Keywords:
Leishmaniasis
Leishmania amazonensis
N, N′, N″-trisubstituted guanidine derivatives
In vivo leishmanicidal activity
Hepatoprotective effect

ABSTRACT

Leishmaniasis is a group of diseases caused by protozoan parasites from the genus *Leishmania*. There are estimated 1.3 million new cases annually with a mortality of 20,000–30,000 per year, when patients are left untreated. Current chemotherapeutic drugs available present high toxicity and low efficacy, the latter mainly due to the emergence of drug-resistant parasites, which makes discovery of novel, safe, and efficacious antileishmanial drugs mandatory. The present work reports the synthesis, characterization by ESI-MS, ^{1}H and ^{13}C NMR, and FTIR techniques as well as *in vitro* and *in vivo* evaluation of leishmanicidal activity of guanidines derivatives presenting lower toxicity. Among ten investigated compounds, all being guanidines containing a benzoyl, a benzyl, and a substituted phenyl moiety, **LQOF-G2** ($IC_{50\text{-ama}}$ 5.6 μM; SI = 131.8) and **LQOF-G7** ($IC_{50\text{-ama}}$ 7.1 μM; SI = 87.1) were the most active against *L. amazonensis* intracellular amastigote, showing low cytotoxicity to the host cells according to their selectivity index. The most promising compound, **LQOF-G2**, was further evaluated in an *in vivo* model and was able to decrease 60% of the parasite load in foot lesions at a dose of 0.25 mg/kg/day. Moreover, this guanidine derivative demonstrated reduced hepatotoxicity compared to other leishmanicidal compounds and did not show nephrotoxicity, as determined by the analyses of biomarkers of hepatic damage and renal function, which make this compound a potential new hit for therapy against leishmaniasis.

Abbreviations: ACN, acetonitrile; $Bi(NO_3)_3 \cdot 5H_20$, bismuth(III) nitrate pentahydrate; Et_3N, triethylamine; DMF, dimethylformamide; NMR, Nuclear Magnetic Resonance; DEPT, Distortion less enhancement by polarization transfer; $CDCl_3$, deuterated chloroform; ESI-MS, Electrospray Ionization Mass Spectrometry; FTIR, Fourier-transform infrared spectroscopy; AmpB, Amphotericin B; MNRET, Micronucleated reticulocytes; PBS, Phosphate Buffered Saline; ALT, alanine aminotransferase; AST, aspartate aminotransferase; ALP, alkaline phosphatase.

* Corresponding author. Laboratório de Química Orgânica Fina, Departamento de Química e Biologia, Faculdade de Ciências e Tecnologia, Universidade Estadual Paulista – UNESP, Campus de Presidente Prudente, Rua Roberto Simonsen, 305, 19060-900, Presidente Prudente, SP, Brazil.
** Corresponding author.
E-mail addresses: marcia.graminha@unesp.br (M.A.S. Graminha), eduardo.gonzalez@unesp.br (E.R.P. González).
[1] Rafael Dias do Espírito Santo and Ángela María Arenas Velásquez contributed equally to this work.

https://doi.org/10.1016/j.ejmech.2019.03.032
0223-5234/

1. Introduction

Leishmaniasis is a complex of diseases that comprises a wide spectrum of clinical manifestations, including visceral, cutaneous and mucocutaneous leishmaniasis. It is caused by more than 20 species of the genus *Leishmania* (Protozoa: Kinetoplastida: Trypanosomatidae) that are transmitted through sandflies (Diptera: Psychodidae: Phlebotominae). These parasitic diseases affect mainly poor people in Africa, Asia and Latin America, and the different disease manifestations are determined by the parasite species and the host immune system. There are estimated 1.3 million new cases annually resulting in 20–30 000 deaths [1].

Pentavalent antimonials, paromomycin, amphotericin B and miltefosine are the commonly used drugs, which require long periods of administration and can have serious side effects. Moreover, drug resistant parasites also contributes to the ineffectiveness of these few therapeutic options [2,3], calling urgently for the development of new, safe and effective drugs against leishmaniasis [4,5].

Guanidines are frequently found in nature and used [6] for syntheses of organic compounds including quinazolines, oxazolidinones, lactones, carbonates and urethanes [7–19].

Guanidine derivatives show several biological effects [20–23], such as cardiovascular dilatation [24], as well as antihistaminic [25], anti-inflammatory [26,27], antidiabetic [28], antibacterial [29], antifungal [29], antiprotozoal/antiparasitic [30–33] and antiviral activity [34–37]. Several compounds with guanidine-moiety are also studied for the treatment of neglected tropical diseases [38], and some studies have tested the effectiveness of guanidines against leishmaniasis [31–33,38–42].

The present work presents synthesis, structural characterization, *in vitro* and *in vivo* antileishmanial activity of ten *N, N′, N″*-trisubstituted guanidine derivatives.

2. Results and discussion

2.1. Synthesis

In a first step, thioureas were synthetized (Scheme 1) as intermediates for the subsequent synthesis of guanidines **LQOFG-1** to **LQOFG-10** using the reported procedure [20,43–45]. In order to form compounds **LQOFG-1** to **LQOFG-10**, the thioureas were reacted with benzylamine (Scheme 2).

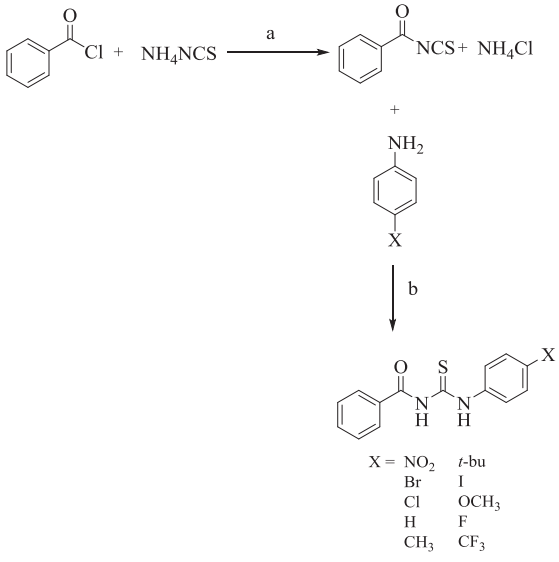

[a]Reagents and conditions: (a) ACN, 75°C, 1h; (b) ACN, 75°C, 2h.

Scheme 1. Synthesis of thioureas. [a]Reagents and conditions: (a) ACN, 75 °C, 1 h; (b) ACN, 75 °C, 2 h.

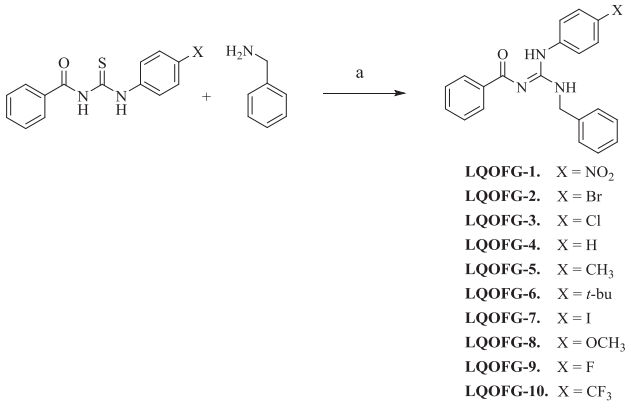

[a]Reagents and conditions: (a) $Bi(NO_3)_3 \cdot 5H_2O$, Et_3N, DMF, 130°C, 24h

Scheme 2. Synthesis of guanidines **LQOFG-1** to **LQOFG-10**. [a]Reagents and conditions: (a) $Bi(NO_3)_3 \cdot 5H_2O$, Et_3N, DMF, 130 °C, 24 h.

2.1.1. Nuclear magnetic resonance spectroscopy (NMR) analysis

^{1}H NMR spectra of guanidines **LQOFG-1** to **LQOFG-10** showed the aromatic hydrogens of the benzoyl moiety, *H10*, *H11* and *H12*, around 8.3, 7.4 and 7.5 ppm, respectively (except for *H10* of **LQOFG-10**, which was at 7.94 ppm). The aromatic hydrogens of the *p*-substituted *N*-phenyl showed chemical shifts of 7.0–7.4 (*H4*) and 6.9–8.2 ppm (*H5*), depending on the nature of the *p*-substituent group. The chemical shifts of the two NH hydrogens were usually observed at ~5 and 12 ppm as broad signals with low intensity resulting from the rapid configurational interconversion between E/Z isomers [20,44].

Other evidence of the guanidine formation is the appearance of methylene and aromatic hydrogens of the benzyl moiety. Table 1 shows representative chemical shifts (ppm) in the ^{1}H NMR spectra for compounds **LQOFG-1** to **LQOFG-10.** Fig. 1 shows the ^{1}H

Table 1
Representative chemical shifts (ppm) obtained by ^{1}H NMR (400 MHz; $CDCl_3$) of compounds **LQOFG-1** to **LQOFG-10**. (More detailed data is described in Experimental part).

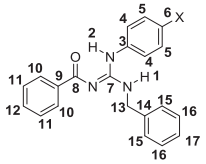

X	*H1*	*H2*	*H4*	*H5*	*X*	*H10*	*H12*	*H13*	*H15*
NO_2	5.99	12.63	7.36	8.23		8.29	7.50	4.92	7.42
Br	5.45	12.15	7.14	7.53		8.29	7.56	4.85	7.41
Cl	5.44	12.16	7.21	7.42		8.29	7.56	4.85	7.40
H	5.26	12.22	7.30	7.44	7.42	8.30	7.50	4.82	7.38
CH_3	5.18	12.05	7.20	7.16	2.35	8.28	7.47	4.78	7.34
t-bu	5.27	12.09	7.19	7.40	1.31	8.27	7.47	4.80	7.36
I	5.16	12.21	7.02	7.70		8.25	7.49	4.76	7.36
OCH_3	5.06	11.93	7.19	6.92	3.81	8.28	7.46	4.77	7.35
F	5.08	12.09	7.09	7.25		8.26	7.46	4.77	7.34
CF_3	4.76	9.16	7.43	8.12		7.94	7; 61	4.59	7.37

Obs. Data of compounds LQOFG-1 to LQOFG-10 in the successive order.

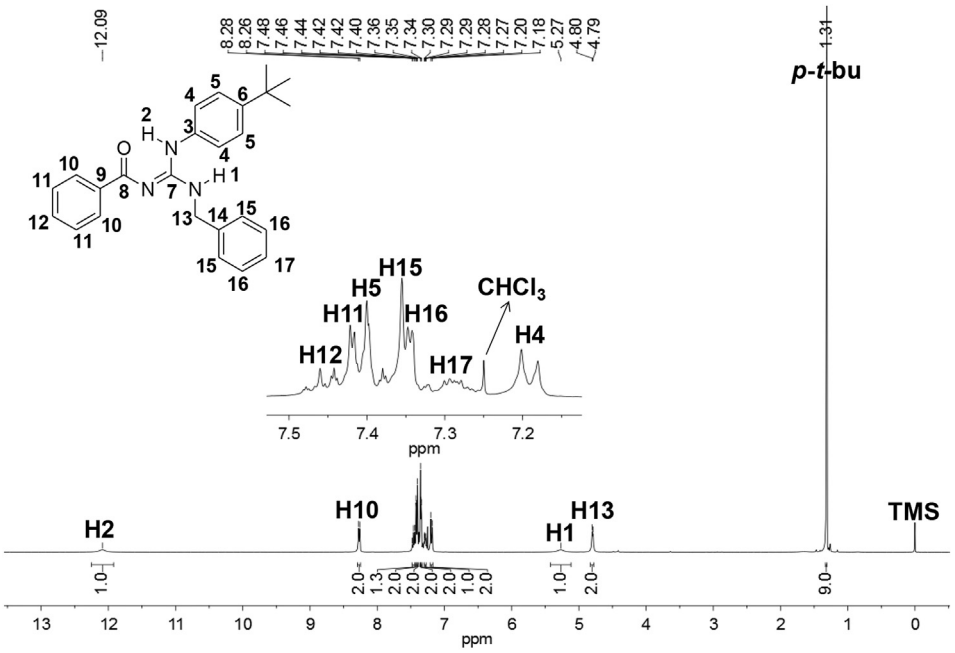

Fig. 1. ^{1}H NMR spectrum of **LQOFG-6**.

NMR spectrum of **LQOFG-6** as a representative of this series of compounds. All ^{1}H NMR spectra are available in supplementary material section.

^{13}C NMR spectra of compounds **LQOFG-1** to **LQOFG-10** also clearly proof the formation of the guanidines by displaying signals related to all three moieties inserted into the molecules. Additional evidence of the compound's formation is the observation of the signals around 158 ppm, characteristic for guanidine carbon (*C7*). The aromatic carbons were observed in the 115–150 ppm region and the carbonyl carbon (*C8*) showed the characteristic shift of around 178 ppm. Table 2 shows representative chemical shifts (ppm) in the ^{13}C NMR spectra for compounds **LQOFG-1** to **LQOFG-10**. Figs. 2 and 3 show ^{13}C NMR and DEPT 135 spectra of **LQOFG-6**, respectively, as examples for this series of compounds. All other ^{13}C NMR spectra are available in supplementary material section.

2.1.2. Electrospray ionization mass spectrometry (ESI-MS) analysis

Compounds **LQOFG-1** to **LQOFG-10** were also studied by mass spectrometry with electrospray ionization in the positive ion mode (ESI(+)-MS). All compounds were identified by the detection of their intact protonated molecules, which were selected and further fragmented via ESI(+)-MS/MS experiments. Fig. 4 shows the HRESI (+)-MS and ESI(+)-MS/MS spectra of the compound **LQOFG-9** (*m/z* 348.1519 $[M+H]^{+}$) as a prototype spectra of this series of compounds.

Compounds **LQOFG-1** to **LQOFG-10** yielded fragment ions at *m/z* 77, 91, 105 and 122, corresponding to phenyl, tropylium, and benzoyl cations, as well as protonated benzamide, respectively (Fig. 4).

The fragment ion at *m/z* 91 is generated by protonation at the alkyl nitrogen, followed by the simple neutral loss of the respective *N*-(*p*-substituted)phenyl-*N*– (benzoyl)guanidines (Scheme 3), and yields the base peak for all compounds with benzyl moiety (with an exception of **LQOFG-1**, where the observed base peak was *m/z* 122).

The fragment ions at *m/z* 105 and 122 are generated by protonation of the amide nitrogen. Formation of benzoyl cation (*m/z* 105) is associated with neutral loss of the *N*-(*p*-substituted)phenyl-*N*-(benzyl)guanidine, and the protonated benzamide (*m/z* 122) involves elimination of a neutral molecule of *N*-(*p*-substituted) phenyl-*N*-(benzyl)carbodiimide. Fragment ions corresponding to the neutral loss of benzamide (*m/z* 227) shown in Fig. 4 are also present at lower intensities for these compounds (Scheme 4).

2.1.3. Fourier-transform infrared spectroscopy (FTIR) measurements

Formation of the compounds **LQOFG-1** to **LQOFG-10** was also confirmed by FTIR spectra through the disappearance of the absorption band at ~ 1262 cm^{-1} associated to *v* (C═S) stretch of the starting thioureas and by appearance of the absorption band at ~ 1566 cm^{-1} characteristic of *v* (C═N) stretch.

Furthermore, the compounds showed absorption bands in the region of 3200–3400 cm^{-1} typical of the *v* (N–H) stretch. In addition, bands were also observed in the 3010-3100 cm^{-1} and 1590-1610 cm^{-1} regions, associated to aromatic *v* (C–H) and *v* (C–C) stretch, respectively. Finally, the absorption bands in the 1630-1730 cm^{-1} region were assigned to *v* (C═O) stretch of carbonyl group [20].

2.2. Evaluation of anti-leishmanial in vitro activity and in vivo mutagenicity [46,47] and activity

2.2.1. In vitro activity evaluation of compounds LQOFG-1 to LQOFG-10

Several guanidine derivatives have been investigated and anti-parasitic, antibacterial, antifungal and anti-HIV effects have been demonstrated [23,31–33,38–42,48–51]. The anti-leishmanial potential of the ten compounds **LQOFG-1** to **LQOFG-10** was evaluated against promastigote and intracellular amastigote forms of *L. amazonensis*, and their cytotoxic effect on host macrophages was tested. All tested compounds showed anti-promastigote activity ranging from 7 to 26 μM. Except for **LQOFG-4**, the other nine compounds showed activity against the intracellular amastigotes, the most clinically relevant stage of *Leishmania* parasites. Only **LQOFG-4** and **LQOFG-10** showed a cytotoxic effect on the host cells, while all others showed no cytotoxicity against macrophages (half-maximal cytotoxicity concentration >500 μM).

Considering the anti-amastigote activity, the data showed that compounds **LQOFG-2** ($IC_{50\text{-ama}} = 5.6$ μM) and **LQOFG-7** ($IC_{50\text{-}}$

Table 2
Representative chemical shifts (ppm) obtained by ^{13}C NMR (400 MHz; $CDCl_3$) of compounds **LQOFG-1** to **LQOFG-10**. (More detailed data is described in Experimental part).

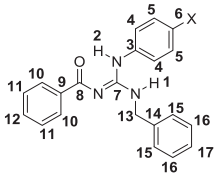

X	C3	C4	C5	X	C7	C8	C10	C12	C13	C15	C16
NO_2	142.6	123.6	125.8		156.9	177.7	129.0	132.0	45.1	127.8	127.9
Br	142.2	127.4	133.1		158.1	177.5	128.9	131.6	44.8	127.7	128.8
Cl	134.1	127.1	131.5		158.2	177.5	130.1	132.5	44.8	127.7	128.9
H	133.6	125.7	127.1		158.7	177.7	129.2	131.4	45.4	127.7	128.9
CH_3	136.0	130.8	125.9	21.2	159.1	177.8	129.3	131.3	45.3	127.7	128.9
t-bu	133.2	125.5	127.2	34.8	159.1	177.9	129.3	131.4	45.3	127.7	128.9
I	133.2	127.9	127.3		158.4	178.0	129.3	131.5	45.4	127.7	129.0
OCH_3	–	122.2	115.3	55.5	158.7	177.7	129.2	131.1	45.2	127.7	128.8
F	128.2	129.1	127.0		159.0	177.9	129.2	131.3	45.3	127.7	128.8
CF_3	–	127.5	125.7	57.0	156.5	177.5	128.9	131.7	45.6	127.9	128.7

Obs. Data of compounds LQOFG-1 to LQOFG-10 in the successive order. (–) Signal not observed.

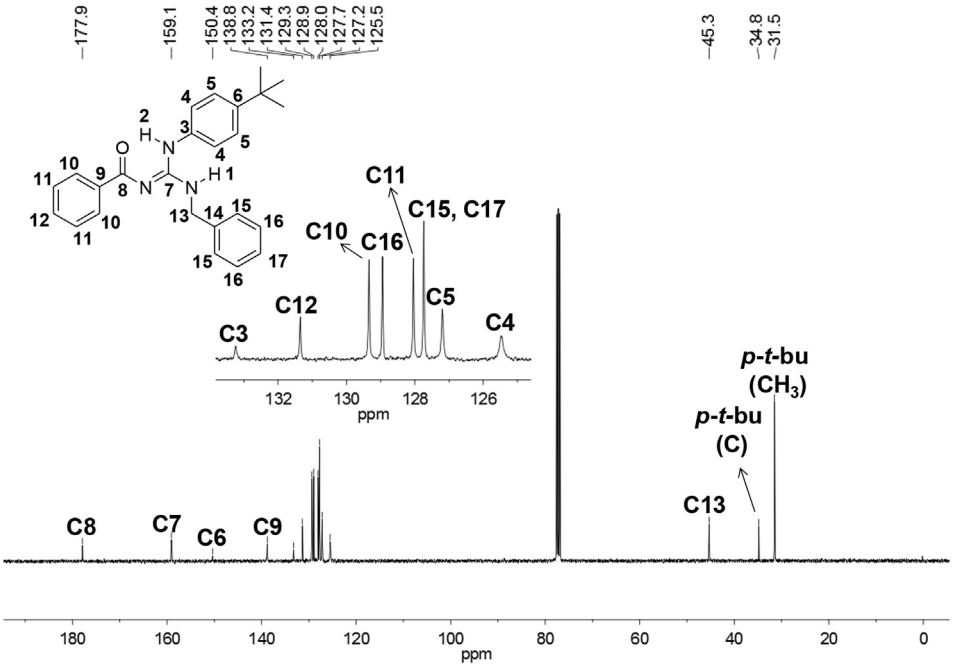

Fig. 2. ^{13}C NMR spectrum of **LQOFG-6**.

$_{ama}$ = 7.1 μM) were the most efficacious in macrophage parasite clearance (Table 3, Fig. 5) and present similar potency when compared to pentamidine ($IC_{50\text{-}ama}$ = 5.1 μM) and AmpB ($IC_{50\text{-}ama}$ = 4.9 μM). Regarding the selectivity towards the parasite rather than to the macrophages, **LQOFG-2** (SI_{ama} = 131.8) and **LQOFG-7** (SI_{ama} = 87.1) were twenty-eight- and eighteen-times more selective than AmpB (SI_{ama} = 4.7). These results indicate that **LQOFG-2** and **LQOFG-7** could be developed into a therapeutic alternative for the treatment of leishmaniasis that could spare the patients the severe side effects presented by the currently used drugs. Although the good selectivity index of compounds **LQOFG-1**, **LQOFG-3**, **LQOFG-5**, **LQOFG-6**, **LQOFG-8** and **LQOFG-9,** makes them promising candidates for leishmaniasis treatment, their anti-amastigote activity ($IC_{50\text{-}ama}$ > 19 μmol L^{-1}) does not meet the hit criteria herein adopted ($IC_{50\text{-}ama}$ < 10 μM). Finally, compound **LQOFG-4**, showed high toxicity to macrophages and no anti-amastigote activity.

Regarding the infection index (percentage of infected cells/number of the intracellular parasites per infected macrophage), treatment with 25 μM concentration of **LQOFG-2, LQOFG-7**, **LQOFG-9** and **LQOFG-3** caused a reduction of 86, 78, 70 and 19%, respectively, in the number of intracellular amastigotes (Fig. 5). **LQOFG-2** was able to reduce the infection as effective as pentamidine (81%) and AmpB (84%). These data suggest the high potential of **LQOFG-2**, **LQOFG-7** and **LQOFG-9** in reducing the number of parasites in *Leishmania* infected macrophages. The compounds

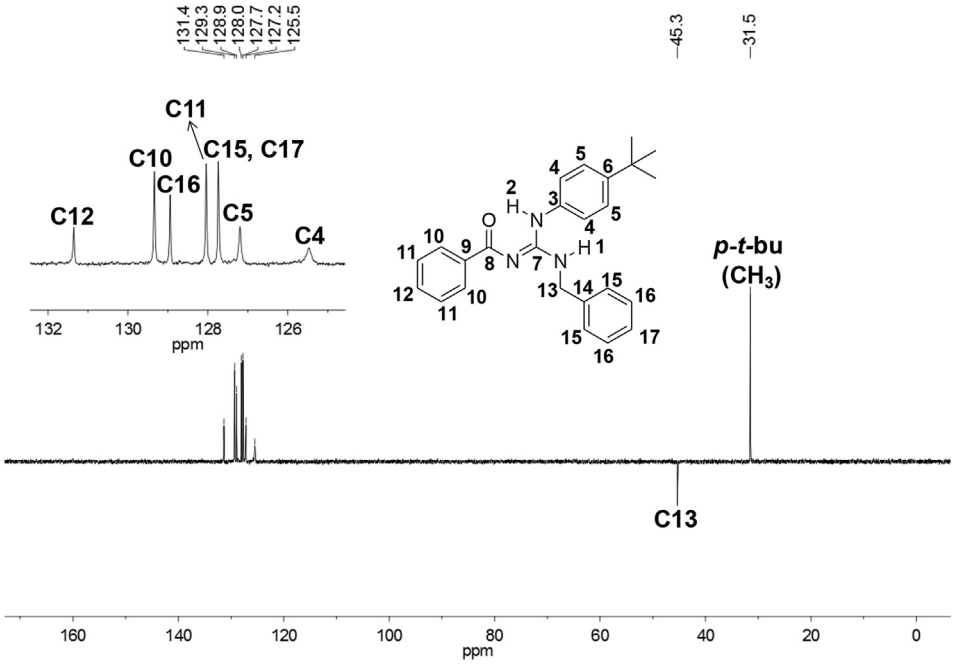

Fig. 3. DEPT 135 spectrum of **LQOFG-6**.

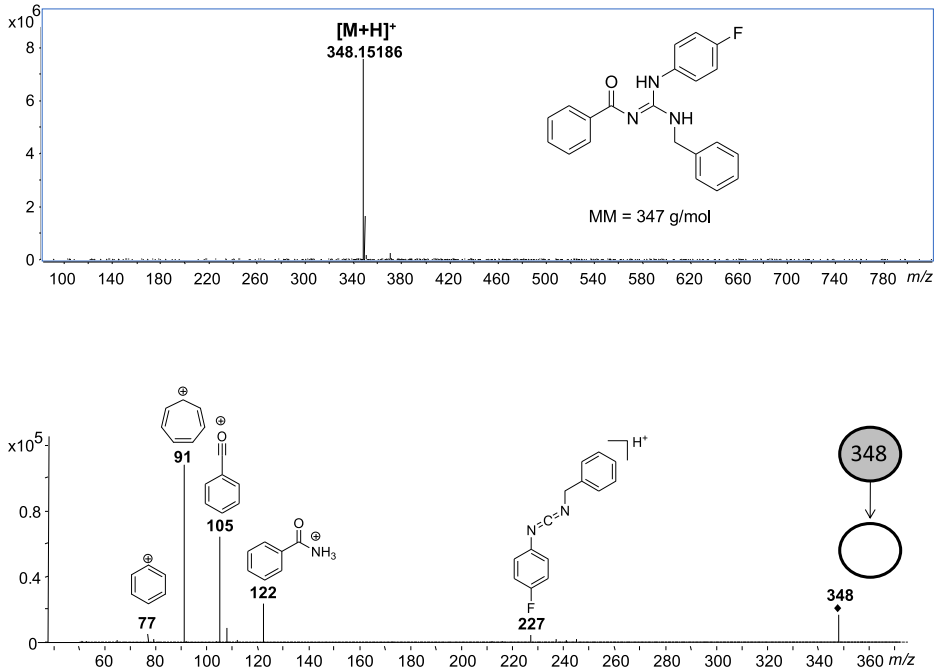

Fig. 4. ESI(+)-MS (up) and ESI(+)-MS/MS (down) spectra of **LQOFG-9**.

containing halogen atoms displayed the ability to reduce macrophage infection following the below potency order (the most active to the less active):

LQOFG-2 (Br) > **LQOFG-7** (I) > **LQOFG-9** (F) > **LQOFG-3** (Cl)

In addition, for all studied compounds the anti-amastigote activity (IC_{50}-μM-data in bold) suggests that the substituent (X) might be contributing to the potency as follows:

G2(Br) **5.6** ≅ G7(I) **7.1** > G6(*t*-Bu) **17.2** ≅ G9(F) **19.0** ≅ G8(CH_3O) **21.1** ≅ G10(CF_3) **21.4** ≅ G1(NO_2) **22.1** ≅ G5(CH_3) **24.2** > G3(Cl) **41.2**

Considering compound **LQOFG-4** (X = H) as a reference, it is reasonable to assume that the presence of a substituent in the fourth position of the aniline moiety is crucial for the anti-leishmanial activity of the investigated N1-benzoyl-N2-benzyl guanidines, with Br and I being favorable for a higher anti-amastigote activity.

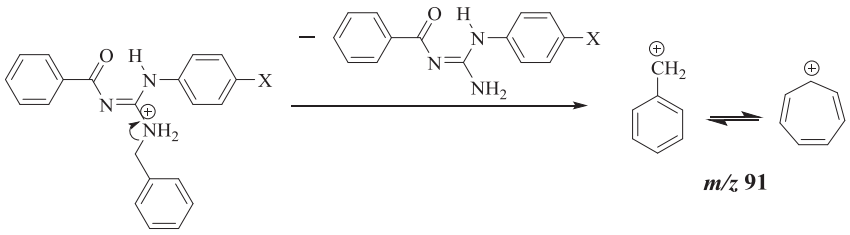

Scheme 3. Formation of the fragment ion at *m/z* 91.

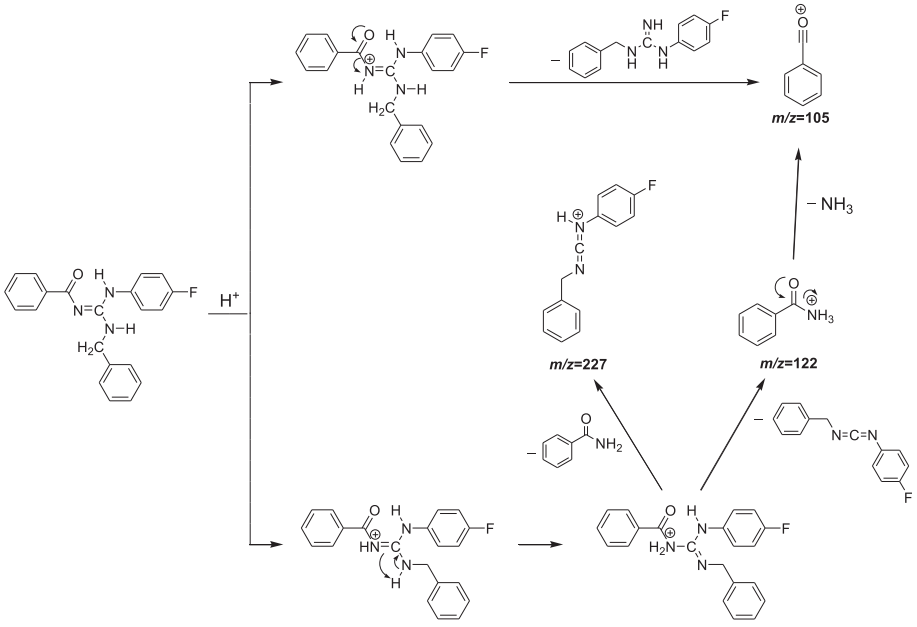

Scheme 4. Proposal for the fragmentation pathway of the compounds **LQOFG-1** to **LQOFG-10** (example for **LQOFG-9**).

Table 3
Antiparasitic activities ($IC_{50\text{-pro/ama}}$, half-maximal inhibitory concentration, μM), mammalian cell toxicity (CC_{50}, half-maximal cytotoxicity concentration, μM) and safety index ($SI = CC_{50}/IC_{50}$) of the guanidine compounds. The SI values ≥ 10 in bold indicate promising compounds, i.e., those with low mammalian toxicity and high toxicity to parasites. Each value is the mean of three experiments performed in triplicate ± standard deviation. pro: promastigote, ama: amastigote.

		Leishmania amazonensis				Macrophage		Safety Index	
Compound	X	$IC_{50\text{-pro}}$	SD	$IC_{50\text{-ama}}$	SD	CC_{50}	SD	promastigote	amastigote
LQOFG-1	NO_2	11.5	0.7	22.1	3.3	801.9	0.3	**69.7**	**36.4**
LQOFG-2	Br	19.6	0.2	5.6	2.5	737.9	1.4	**37.7**	**131.8**
LQOFG-3	Cl	19.7	0.1	41.2	4.1	827.4	1.5	**42.0**	**20.1**
LQOFG-4	H	22.6	1.1	ND		35.9	5.6	1.6	ND
LQOFG-5	CH_3	20.9	0.5	24.2	5.2	876.1	1.7	**41.9**	**36.2**
LQOFG-6	*t*-Bu	25.9	0.9	17.2	2.1	1118.9	105.4	**43.2**	**65.0**
LQOFG-7	I	15.9	0.9	7.1	0.8	618.7	70.2	**38.9**	**87.1**
LQOFG-8	CH_3O	25.4	1.5	21.1	3.6	836.6	1.6	**32.9**	**39.6**
LQOFG-9	F	21.9	1.8	19.0	4.6	865.5	1.7	**39.5**	**45.5**
LQOFG-10	CF_3	6.8	0.2	21.4	0.6	18.6	2.9	2.7	0.8
Pentamidine		7.6	0.1	5.07	1.14	35.7	6.8	4.7	7.0
AmpB		3.2	0.1	4.92	0.14	23.1	2.5	7.2	4.7

For the compound **LQOFG-2 (Br)**, herein the best anti-leishmanial candidate, a strong predominance of a '*Z*' isomer was observed by NMR [20]. This was, however, not the case with compound **LQOFG-1 (NO_2),** where equal populations of isomers '*Z*' and '*E*' were found [20].

Therefore, the presence of these groups in the structure of guanidines, can probably modify the binding strength to possible targets in the parasite by charge and conformational effects.

Guanidines as well as some analogues of marine guanidine alkaloids showed a broad spectrum of action for the treatment of different infectious diseases including for leishmaniasis [20,22,23,31–33,39–42,48]. Indeed, the polymeric guanidine AKACID Plus® was able to decrease skin infections caused by methicillin-resistant *Staphylococcus aureus* through topical application [52] and several *bis*guanidine-indenes have exhibited anti-*Trypanosoma brucei* activity *in vivo* mouse models [51,53], reinforcing the potential of guanidine compounds. Thus, in order to further evaluate the *in vivo* leishmanicidal potential of the

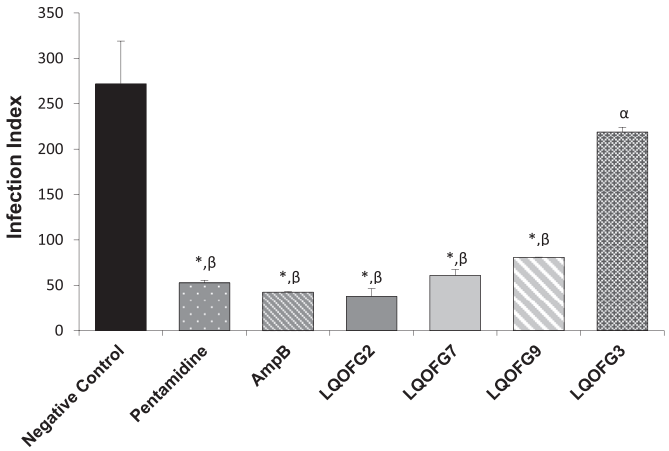

Fig. 5. *In vitro* effect of **LQOFG-2, LQOFG-7, LQOFG-9** and **LQOFG-3** on *L. amazonensis* intracellular amastigotes. The infection index was calculated after 72 h of treatment with 25 μM of each guanidines, pentamidine and AmpB. The negative control is untreated *L. amazonensis* intracellular amastigotes. Data are expressed as average ± SD. *,α: Statistically significant difference relative to negative control (*: $p < 0.001$; α: $p < 0.05$). β: Statistically significant difference relative to **LQOFG-3** ($p < 0.001$).

guanidine compounds developed herein, **LQOFG-2** was chosen based on the previously-mentioned hit criteria and DNDi recommendations [54] ($IC_{50} < 10\ \mu mol\ L^{-1}$ and $SI \geq 10$).

2.2.2. *In vivo mutagenicity [46,47]of the two compounds (LQOFG-2 and LQOFG-7) with higher activity against intracellular amastigotes*

Determination of *in vivo* mutagenicity was performed for compounds **LQOFG-2** and **LQOFG-7**, the most potent anti-leishmanial guanidine derivatives. Fig. 6 shows the frequency of micronucleated reticulocytes (MNRET) per 2000 cells obtained from animals treated either with hydroxyethylcellulose 0.5% (negative control), cyclophosphamide (positive control) or 25, 50 and 100 mg/kg of **LQOFG-2** and **LQOFG-7**.

The results demonstrated that **LQOFG-2** and **LQOFG-7**, administered at different concentrations, have not induced a significant increase in the frequency of micronuclei in reticulocytes of mice at all tested concentrations, compared to negative control. However, in the animal group exposed to the genotoxic agent cyclophosphamide, the frequency of micronuclei in mice reticulocytes was significantly higher (24 micronucleated reticulocytes) in comparison to the negative control group (5 micronucleated reticulocytes). The substance is considered to be mutagenic when the mutagenic index (MI) is equal to or greater than 2 for at least one of the tested doses [46]. In case of **LQOFG-2** and **LQOFG-7**, the MI was less than 2 in all tested doses and therefore, no mutagenic properties were observed (Table 4).

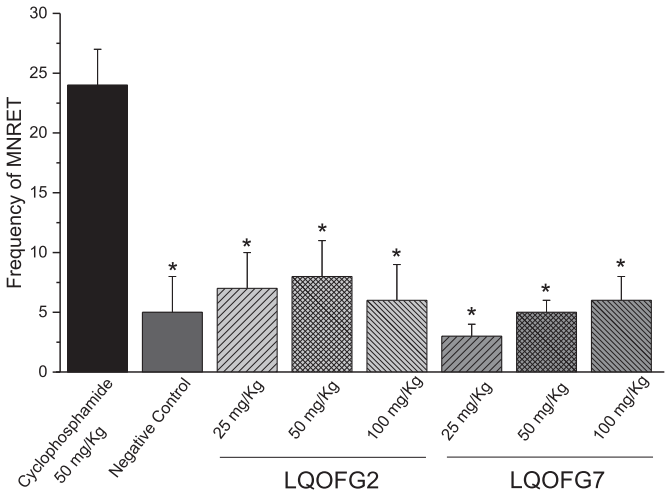

Fig. 6. LQOFG-2 and **LQOFG-7** do not increase the frequency of micronucleated reticulocytes (MNRET). Average frequency and standard deviation of MNRET per 2000 cells from mice treated with cyclophosphamide (positive control), hydroxyethylcellulose (negative control) and 25 mg/kg, 50 mg/kg and 100 mg/kg of guanidine derivatives. *: Statistically significant difference relative to the animals treated with 50 mg/kg of cyclophosphamide ($p < 0.05$).

The mutagenicity evaluation is essential to determinate the drug safety for human use and it is recommended by regulatory agencies. Typically, the test can detect lesions in the structure of the chromosomes as well as changes in the distribution of these chromosomes during the process of cell division. Both lesions are induced by chemicals, through the formation of micronuclei with fragments of DNA or whole chromosomes. During normal erythropoiesis, micronuclei are formed at low frequency, and micronuclei containing erythrocytes are removed rapidly and efficiently from peripheral blood circulation. The presence of micronuclei concomitantly with immature erythrocytes in circulation is an indicator of chromosomal damage [46,47].

2.2.3. *In vivo activity investigation of the best candidate LQOFG-2*

L. amazonensis infected BALB/c mice (six weeks post infection) were daily treated for 15 days with two different doses of **LQOFG-2** (0.13 and 0.25 mg/kg/day) or AmpB (2 mg/kg/day) by intraperitoneal administration. The animals treated with **LQOFG-2** reduced the parasite burden by 46 and 60% at 0.13 and 0.25 mg/kg/day, respectively. AmpB, given at much higher dosage, reduced the parasite load only by 41%, similarly to that obtained with the lowest dose of the tested guanidine compound (Fig. 7).

The **LQOFG-2** treatment also decreased the size of the lesion in both doses in comparison with untreated infected animals and infected animals treated with PBS, and similarly to AmpB at 2 mg/kg/day (Fig. 8). On the other hand, no statistically significant change of weight was observed during the treatment in all analyzed groups.

In order to evaluate the potential toxic effect of **LQOFG-2**, the plasma levels of creatinine and urea (biomarkers of kidney function), AST, ALT, and ALP (biomarkers of hepatic damage), and bilirubin (marker of hepatic function) were monitored. No changes were observed in creatinine (Fig. 9A) and urea plasma levels (Fig. 9B) of all animals, suggesting that both the infection with *L. amazonensis* and/or the treatment with **LQOFG-2** did not cause renal dysfunction. The plasma levels of bilirubin were significantly increased in animals infected with *L. amazonensis*, treated or not with AmpB or with **LQOFG2** (Fig. 9C). Considering that the increases in bilirubin levels were similar among all groups of infected animals, treated or not with **LQOFG-2**, it can be suggested that this

Table 4
Mutagenic index (MI) of **LQOFG-2** and **LQOFG-7** at different doses tested against peripheral mice blood cells. The MI was calculated as the ratio between the micronucleated reticulocytes (MNRET) of tested drug and MNRET of negative control (hydroxyethylcellulose 0.5%).

Compound	Dose (mg/kg)	MNRET	MI
Negative control	–	5 ± 3	–
cyclophosphamide	50	24 ± 3	4.8
LQOFG-2	25	7 ± 3	1.4
	50	8 ± 3	1.6
	100	6 ± 3	1.2
LQOFG-7	25	3 ± 1	0.6
	50	5 ± 1	1.0
	100	6 ± 2	1.2

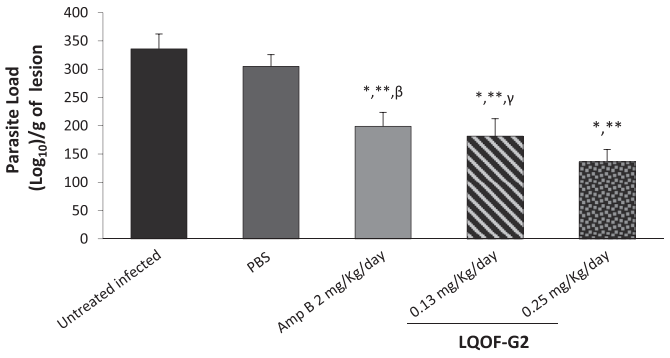

Fig. 7. Parasite load after treatment of *L. amazonensis*-infected BALB/c mice with **LQOFG-2**. Five groups containing five BALB/c mice infected with *L. amazonensis* were treated daily with **LQOFG-2** or AmpB for 15 days. Quantification of tissue parasite load in skin lesions post-treatment was determined by the limiting dilution method. The data are expressed as average ± SD. *: Statistically significant difference relative to the untreated infected group ($p < 0.001$). **: Statistically significant difference relative to the vehicle group − PBS ($p < 0.001$). β,γ: Statistically significant difference relative to the infected group treated with 0.25 mg/kg/day of **LQOFG-2** ($p < 0.01$; $p < 0.25$).

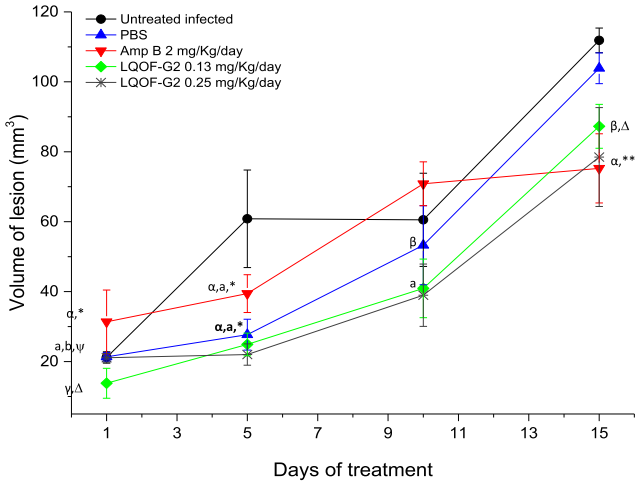

Fig. 8. Reduction of foot lesions in *L. amazonensis*-infected BALB/c mice treated with **LQOFG-2**. Groups of five BALB/c mice infected whit *L. amazonensis* were treated with **LQOFG-2** or AmpB for 15 days. (a) Values of volume of foot lesions were monitored every 5 days to validate the *in vivo* efficacy of **LQOFG-2**. Data points represent the average measurements for 7 groups of 5 mice each. The data are expressed as average of volume (v = D x d x e; D: larger diameter, d: minor diameter, e: thickness) ± SD. α,β,γ: Statistically significant difference relative to the untreated infected group ($p < 0.001$; $p < 0.01$; $p < 0.05$). a,b: Statistically significant difference relative to the vehicle group − PBS ($p < 0.001$; $p < 0.01$). *,**,Δ: Statistically significant difference relative to the infected group treated with 2 mg/kg/day of AmpB ($p < 0.001$; $p < 0.01$; $p < 0.05$). ψ: Statistically significant difference relative to the infected group treated with 0.13 mg/kg/day of **LQOFG-2** ($p < 0.05$).

increase in bilirubin may be due to the harmful impacts of *L. amazonensis* infection on liver function, having no relationship with drug hepatotoxicity. Corroborating the findings about the detrimental impacts of *L. amazonensis* infection in liver, increased plasma levels of ALP, AST, and ALT were observed in infected animals, treated or not with PBS (Fig. 9D–F), indicating that the infection caused damage in hepatic cells, as previously observed [55]. The treatment of infected animals with AmpB decreased the plasma levels of ALP and ALT, suggesting that this treatment partially prevented liver damage. Treatments with **LQOFG-2** also decreased the hepatic damage like AmpB: although the treatment was not effective in reducing the AST levels (Fig. 9E), reductions in ALP (Fig. 9D) and in ALT (Fig. 9F) levels were observed in all tested doses of **LQOFG-2**. It is worth mentioning that, in infected animals treated with 0.13 or 0.25 mg/kg/day **LQOFG-2**, the ALP and ALT levels were similar those values found in uninfected animals, highlighting the protective effect of **LQOFG-2** against the harmful consequences of *L. amazonensis* infection on liver integrity.

Our data indicate that **LQOFG-2** is very efficient due to its excellent biological activity against *L. amazonensis* and might be considered a promising drug candidate for treatment of cutaneous leishmaniasis since **LQOFG-2** showed a high selectivity index, good capacity to decrease parasite burden in *in vivo* experiments and no toxicological/mutagenic effects.

3. Conclusion

In this study, ten benzoyl − benzyl guanidine derivatives were synthetized, out of which compounds **LQOFG-2** and **LQOFG-7** have been found to show highest activity against *L. amazonensis* intracellular amastigote forms. *In vivo* experiments showed that the parasite burden in *L. amazonensis*-infected BALB/c mice was more strongly reduced by **LQOFG-2** when compared to AmpB, the commercial drug used in the treatment of *Leishmania*, although **LQOFG-2** was tested at lower doses than AmpB. Additionally, a reduction in the parasite-induced hepatotoxicity and absence of nephrotoxicity were observed in mice treated with two doses of **LQOFG-2** *in vivo*. **LQOFG-2** and **LQOFG-7** are not mutagenic as evaluated by the micronucleus test. Therefore, the results of the biological evaluation demonstrated that these compounds can be considered as suitable candidates in the search for new drugs for the therapy of leishmaniasis. This is very important considering the high selective index and low toxicity of the synthetic candidate LQOFG-2 and in addition the high infectivity by Leishmania in several countries, as in the case of Brazil, and the inconvenience of the conventional therapy.

4. Experimental section

4.1. Synthesis and analytics

Commercial benzoylchloride, ammonium isothiocyanate, aniline, 4-nitroaniline, 4-bromoaniline, 4-chloroaniline, 4-fluoroaniline, 4-iodoaniline, 4-methoxyaniline, toluidine, 4-*t*-butylaniline, benzylamine, 4-aminobutanol, triethylamine, pentahydrated bismuth nitrate and the solvents *N,N*-dimethylformamide, acetonitrile and dichloromethane were used without previous purification.

Thin layer chromatography (TLC) was performed on silica gel plates and the compounds visualized using iodine reagent.

^{1}H and ^{13}C NMR spectra were recorded on a Bruker Avance III − 400 MHz and a Bruker Avance III − 600 MHz (Bruker, Bremen, Germany). The resonance frequency for ^{1}H NMR was 400.13 MHz and for ^{13}C NMR 100.61 MHz. Chemical shifts for ^{1}H NMR and ^{13}C NMR were referenced to TMS, analysis was performed in $CDCl_3$ and all chemical shifts were reported in ppm. Data are presented as following: chemical shift, multiplicity (s = singlet, d = doublet, dd = doublet of doublet, t = triplet, qua = quadruplet, qu = quintuplet, m = multiplet, br s = broad singlet), integration, and coupling constants (in Hertz).

To obtain ESI(+)-MS data, the samples were diluted in 1 mL of acetonitrile and 1 μL of the solution was injected using an autosampler LC Agilent 1290 (Agilent, California, USA) into the electrospray source of the mass spectrometer Agilent 6550 iFunnel Q-TOF LC/MS (Agilent, California, USA). The mobile phase of the LC was an acetonitrile solution containing 0.1% of formic acid at a flow rate of 0.1 mL/min. The electrospray ionization source operated in positive mode under the following conditions: nebulization gas

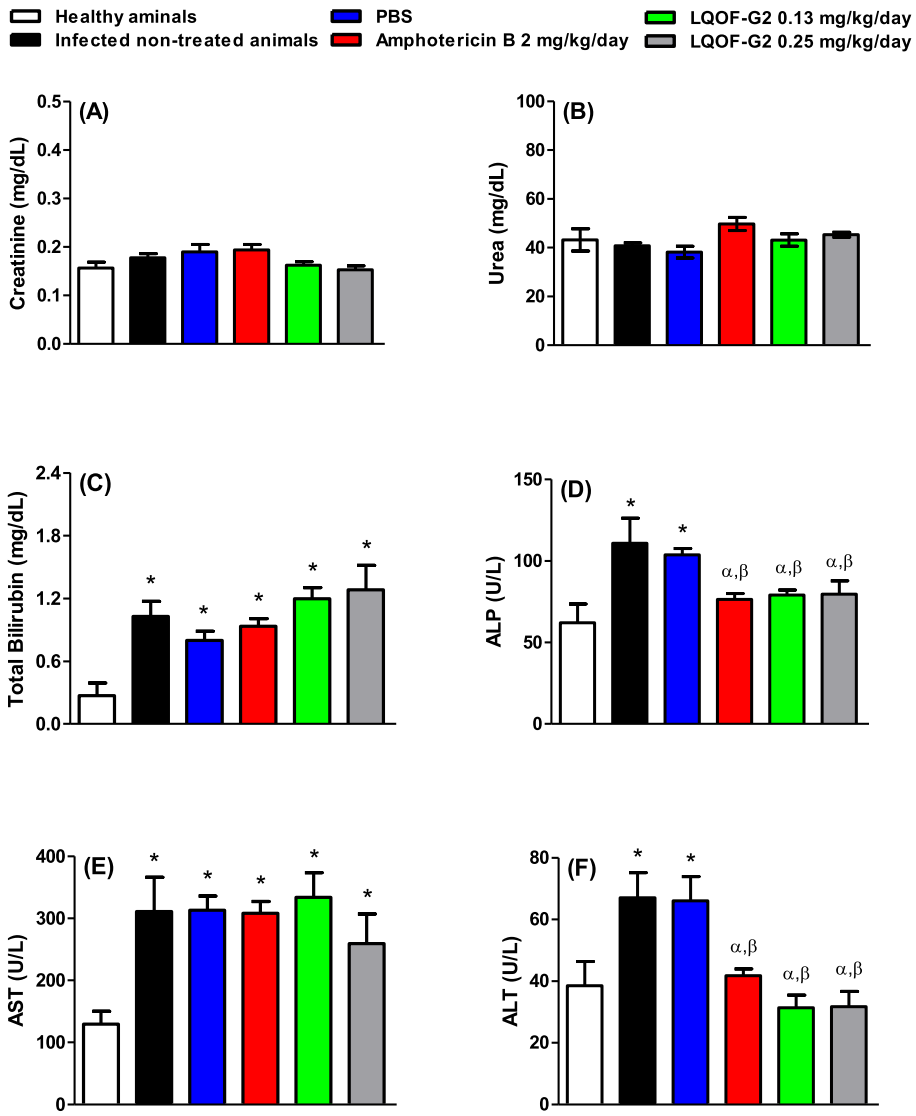

Fig. 9. Plasma levels of biomarkers of renal function and liver damage in BALB/c mice noninfected and infected with *L. amazonensis* and treated with 0.13 or 0.25 mg/kg/day of **LQOFG2**. (**A**) Creatinine levels; (**B**) Urea levels; (**C**) Total bilirubin levels; (**D**) ALP levels; (**E**) AST levels; (**F**) ALT levels. The data are expressed as averages ± SD. *: Statistically significant difference relative to the uninfected animals (healthy animals) ($p < 0.05$); α: Statistically significant difference relative to the untreated infected group ($p < 0.05$); β: Statistically significant difference relative to the vehicle group - PBS ($p < 0.05$).

temperature: 290 °C, capillary voltage: 3500 V, Nozzle Voltage 320 V, dry gas flow: 14 mL/min, nebulization gas pressure: 45 psig, gas auxiliary temperature: 350 °C and auxiliary gas flow: 12 mL/min. The quadrupole analyzer operated in the range of *m/z* 100–1000, fragmentor voltage: 100 V, octupole voltage: 750 V, and acquisition of 1 spectrum/s was obtained with high resolution in TOF up to the fifth decimal place. Formulas were assigned a 1 ppm error using Agilent Mass Hunter Workstation software.

HRESIMS spectra were obtained on a maXis UHR ESI-Qq-TOF mass spectrometer (Bruker Daltonics, Bremen, Germany). Samples were dissolved to 20 μg/mL in MeOH and directly infused into the ESI source at a flow rate of 3 μL/min with a syringe pump. The ESI ion source was operated as follows: capillary voltage: 4.5 kV, nebulizer: 0.4 bar (N_2), dry gas flow: 4 L/min (N_2), and dry temperature: 180 °C. Mass spectra were recorded in the range of *m/z* 50–1900 in the positive-ion mode. The sum formulas were determined using Bruker Compass DataAnalysis 4.1 based on the mass accuracy ($\Delta m/z \leq 5$ ppm) and isotopic pattern matching (SmartFormula algorithm).

The purity of the compounds was determined by HPLC method on UFLC XR Prominence device (Shimadzu Corporation, Tokyo, Japan). Separation was carried out on an Acclaim 120C18, 4.6 × 250 mm, 5 μm HPLC column (Thermo Fisher Scientific) using LC-MS-grade water and acetonitrile as mobile phase A and B, respectively. The sample components were separated and eluted with a linear gradient from 10% to 90% B in 30 min followed by 30 min isocratic step with 90% B and a re-equilibration step. The flow rate was 0.6 mL/min and the column oven temperature was set to 25 °C.

FT-IR data were recorded on a Vector 22 instrument (Bruker, Bremen, Germany) and collected at 25 °C room temperature with 124 scans and spectral resolution of 4 cm^{-1}. Samples mixed in a 1 mg/20 mg ratio with KBr and pressed to tablets.

Melting points (m.p.) were obtained using a WRS-2 Micro Processor Melting-point apparatus. The samples were placed in a capillary tube, and the pre-heating and final ramp temperatures

were selected for 60 °C and 250 °C, respectively. The heating rate used was 4.0 °C/min.

4.1.1. General procedure for the synthesis of guanidines [20,25,43,45].

Benzoyl chloride (1.40 g, 10 mmol) was added to a solution of ammonium isothiocyanate (0.76 g, 10 mmol) in acetonitrile (20 mL) and the resulting mixture was refluxed for 1 h. Then, the reaction solution was filtered for removal of ammonium chloride, and 10 mmol of respective aniline was added. The reaction mixture was refluxed for additional 2 h. The crude product was filtered and washed with cold acetonitrile to generate thioureas. To a solution of 1 mmol of thiourea dissolved in 5 mL of *N,N*-dimethylformamide was added 2 mmol of benzylamine or 4-aminobutanol, 4 mmol of triethylamine and then 1 mmol of $Bi(NO_3)_3 \cdot 5H_2O$. The solution became black after a few minutes and the mixture was heated for 24 h at ~100 °C. After this time, the suspension was filtered through a pad of celite, which was washed with 20 mL of di-chloromethane. The impurity of filtrate was removed via extraction with water (4 × 15 mL), the organic phase dried over anhydrous $MgSO_4$ and evaporated. The crude residue was crystallized from Et_2O/petroleum ether.

*4.1.1.1. (Z)–N-((benzylamino) ((4-nitrophenyl)amino)methylene) benzamide (**LQOFG-1**).* Yield 66%. ^{1}H NMR - 60 °C (400.13 MHz, $CDCl_3$) δ Z isomer = 12.63 (s, 1H), 5.99 (t, 1H), 4.92 (d, 2H). δ E isomer = 11.33 (t, 1H), 8.73 (s, 1H), 4.64 (d, 2H). ^{13}C NMR (100.61 MHz, $CDCl_3$) δ Z isomer = 177.7 (C═O), 156.9 (N═C), 144.2 (C–NO_2), 142.6 (C), 137.8 (C), 134.8 (C), 132.0 (p-CH), 129.0 (2CH), 128.9 (2CH), 127.9 (2CH), 127.8 (2CH), 127.0 (p-CH), 125.8 (2CH), 123.6 (2CH), 45.1 (N–CH_2). δ E isomer = 178.1 (C═O); 157.7 (N═C), 144.1 (C–NO_2), 142.2 (C), 137.2 (C), 129.5 (C), 129.3 (p-CH), 128.3 (2CH), 128.2 (2CH), 127.9 (2CH), 126.9 (2CH), 126.1 (p-CH), 124.7 (2CH), 121.8 (2CH), 45,5 (N–CH_2). FT-IR (KBr) ν 3423, 3061, 3027, 2930, 1630, 1601, 1566, 1505, 1329 e 1109 cm^{-1} HRESIMS *m/z* 375.1449 $[M+H]^+$ (calcd for $C_{21}H_{19}N_4O_3^+$, 375.1452, Δ = 0.7 ppm). Ret. time 34.95 min, purity 95.3%. m.p. 136.6–137.8.

*4.1.1.2. (Z)–N-((benzylamino) ((4-bromophenyl)amino)methylene) benzamide (**LQOFG-2**).* Yield 71%. ^{1}H NMR - 60 °C (400.13 MHz, $CDCl_3$) δ Z isomer = 12.15 (s, 1H), 8.29 (d, 2H), 7.54–7.48 (m, 5H), 7.41–7.35 (m, 5H), 7.14 (d, 2H), 5.45 (t, 1H), 4.85 (d, 2H). δ E isomer = 11.16 (s, 1H). ^{13}C NMR (100.61 MHz, $CDCl_3$) δ = 177.5 (C═O), 158.1 (C═N), 138.2 (C), 137.6 (C), 134.1 (C), 133.1 (2CH), 131.6 (p-CH), 128.9 (2CH), 128.8 (2CH), 128.1 (2CH), 127.7 (2CH + p-CH), 127.4 (2CH), 120.6 (C–Br), 44.8 (N–CH_2). FT-IR (KBr) ν 3432, 3062, 2930, 1601, 1559, 1363 e 1196 cm^{-1} HRESIMS *m/z* 408.0701 $[M+H]^+$ (calcd for $C_{21}H_{19}BrN_3O^+$, 408.0706, Δ = 1.2 ppm). Ret. time 37.52 min, purity 96.5%. m.p. 94.8–96.1 °C.

*4.1.1.3. (Z)–N-((benzylamino) ((4-chlorophenyl)amino)methylene) benzamide (**LQOFG-3**).* Yield 69%. ^{1}H NMR -60 °C (400.13 MHz, $CDCl_3$) δ Z isomer = 12.16 (s, 1H), 8.29 (d, 2H, *J* = 7,6 Hz), 7.56 (t, 1H, *J* = 7,2 Hz), 7.48 (t, 2H, *J* = 7,5 Hz), 7.42–7.37 (m, 6H), 7.31 (m, 1H), 7.21 (d, 2H, *J* = 8,5 Hz), 5.44 (t, 1H, *J* = 5,8 Hz), 4.85 (d, 2H, *J* = 5,8 Hz). δ E isomer = 11.20 (t, 0,1H, *J* = 5,1 Hz), 10.00 (s, 0,1H). ^{13}C NMR (100.61 MHz, $CDCl_3$) δ = 177.5 (C═O), 158.2 (N═C), 138.2 (C), 137.6 (C), 133.6 (C), 132.5 (p-CH), 131.5 (2CH), 130.1 (2CH), 128.9 (2CH), 128.7 (2CH), 128.0 (p-CH), 127.6 (2CH), 127.1 (2CH), 44.8 (N–CH_2). FT-IR (KBr) ν 3435, 3064, 2931, 1601, 1558, 1361 e 1198 cm-1. HRESIMS *m/z* 364.1208 $[M+H]^+$ (calcd for $C_{21}H_{19}ClN_3O^+$, 364.1211, Δ = 0.8 ppm). Ret. time 36.95 min, purity 88.5%. m.p. 87.3–88.5 °C.

*4.1.1.4. (Z)–N-((benzylamino) (phenylamino)methylene)benzamide (**LQOFG-4**).* Yield 89%. ^{1}H NMR (400.13 MHz, $CDCl_3$) δ = 12.22 (br, 1H), 8.30 (br, 2H), 7.50 (t, *J* = 6,8 Hz, 1H), 7.44 (m, 5H), 7.37 (d, 4H), 7.33–7.30 (m, 3H), 5.26 (br, 1H), 4.82 (br, 2H). ^{13}C (100.61 MHz, $CDCl_3$) δ = 177.7 (C═O), 158.7 (N═C), 138.6 (C), 136.0 (C), 131.4 (p-CH), 130.1 (C–H), 129.2 (2CH), 128.9 (2CH), 128.0 (2CH), 127.7 (2CH), 127.6 (p-CH), 127.1 (2CH), 125.7 (2CH), 45.4 (N–CH_2). FT-IR (KBr) ν 3413, 3168, 3067, 2918, 1601, 1566, 1355 e 1198 cm^{-1}. HRESIMS *m/z* 330.1601 $[M+H]^+$ (calcd for $C_{21}H_{19}N_3O^+$, 330.1601, Δ = −0.1 ppm). Ret. time 35.12 min, purity 93.5%. m.p. 94.4–94.9 °C.

*4.1.1.5. (Z)–N-((benzylamino) (p-tolylamino)methylene)benzamide (**LQOFG-5**).* Yield 53%. ^{1}H NMR (400.13 MHz, $CDCl_3$) δ = 12.05 (br, 1H), 8.27 (d, *J* = 7,1 Hz, 2H), 7.46 (t, *J* = 7,0 Hz, 1H), 7.41 (t, *J* = 7,3 Hz, 2H), 7.33 (d, *J* = 4,5 Hz, 4H), 7.29 (dd, *J* = 8,7, 4,5 Hz, 1H), 7.20 (d, *J* = 8,1 Hz, 2H), 7.15 (d, *J* = 8.0 Hz, 2H), 5.18 (br, 1H), 4,78 (br, 2H), 2,35 (s, 3H). ^{13}C NMR (100.61 MHz, $CDCl_3$) δ = 177.8 (C═O), 159.1 (N═C), 138.7 (C), 137.3 (C), 133.2 (C), 131.3 (p-CH), 130.8 (2CH), 129.3 (2CH), 128.9 (2CH), 128.0 (2CH), 127.7 (2CH + p-CH), 125.9 (2CH), 45.3 (N–CH_2), 21.2 (p-CH3). FT-IR (KBr) ν 3412, 3212, 3027, 2818, 1651, 1601, 1556, 1358 e 1201 cm^{-1}. HRESIMS *m/z* 344.1758 $[M+H]^+$ (calcd for $C_{22}H_{22}N_3O^+$, 344.1757, Δ = −0.1 ppm). Ret. time 36.67 min, purity 96.0%. m.p. 91.2–91.7 °C.

*4.1.1.6. (Z)–N-((benzylamino) ((4-(tert-butyl)phenyl)amino)methylene)benzamide (**LQOFG-6**).* Yield 70%. ^{1}H NMR (400.13 MHz, $CDCl_3$) δ = 12,09 (br, 1H), 8,27 (d, *J* = 7,1 Hz, 2H), 7,48–7,44 (m, 1H), 7,42 (m, 2H), 7,40 (m, 2H), 7,35 (m, 4H), 7,29 (m, 1H), 7,19 (d, *J* = 8,5 Hz, 2H), 5,27 (br, 1H), 4.79 (d, *J* = 5.3 Hz, 2H), 1.31 (s, 9H); ^{13}C NMR (100.61 MHz, $CDCl_3$) δ = 177.9 (C═O), 159.1 (N═C), 150.4 (C), 138.8 (C), 133.2 (C), 131.4 (p-CH), 129.3 (2CH), 128.9 (2CH), 128.0 (2CH), 127.7 (2CH + p-CH), 127.2 (2CH), 125.5 (2CH), 45.3 (N–CH_2), 34.8 [p-*t*-bu (C)], 31.5 [p-*t*-bu (CH3)]. FT-IR (KBr) ν 3323, 3060, 2959, 1696, 1595, 1566, 1364 e 1209 cm^{-1}. HRESIMS *m/z* 386.2227 $[M+H]^+$ (calcd for $C_{25}H_{28}N_3O^+$, 386.2227, Δ = −0.0 ppm). Ret. time 41.04 min, purity 95.8%. m.p. 124.4–125.7 °C.

*4.1.1.7. (Z)–N-((benzylamino) ((4-iodophenyl)amino)methylene) benzamide (**LQOFG-7**).* Yield 50%. ^{1}H NMR (400.13 MHz, $CDCl_3$) δ = 12.21 (br, 1H), 8.25 (br, 2H), 7.71 (d, *J* = 7.9 Hz, 2H), 7.49 (t, *J* = 6.8 Hz, 1H), 7.42 (t, *J* = 7.6 Hz, 2H), 7.35 (m, 4H), 7.30 (m, 1H), 7.02 (br, 2H), 5.16 (br, 1H), 4.76 (br, 2H); ^{13}C NMR (100.61 MHz, $CDCl_3$) δ = 178.0 (C═O), 158.4 (N═C), 139.2 (C), 138.3 (C), 131.5 (p-CH), 129.3 (2CH), 129.0 (2CH), 128.0 (2CH), 127.9 (2CH), 127.7 (2CH + p-CH), 127.3 (2CH), 45.4 (N–CH_2). FT-IR (KBr) ν 3353, 3055, 2931, 1654, 1603, 1566, 1508, 1354 e 1207 cm- [1]. HRESIMS *m/z* 456.0566 $[M+H]^+$ (calcd for $C_{21}H_{19}IN_3O^+$, 456.0567, Δ = −0.3 ppm). Ret. time 38.35 min, purity 90.9%. m.p. 99.6–101.0 °C.

*4.1.1.8. (Z)–N-((benzylamino) ((4-methoxyphenyl)amino)methylene) benzamide (**LQOFG-8**).* Yield 85%. ^{1}H NMR (400.13 MHz, $CDCl_3$) δ = 11.93 (br, 1H), 8.27 (d, *J* = 7.4 Hz, 2H), 7.46 (m, 1H), 7.41 (m, 2H), 7.33 (m, 4H), 7.29 (m, 1H), 7.19 (d, *J* = 8.6 Hz, 2H), 6.92 (dt, *J* = 8.9 Hz, 2H), 5.06 (br, 1H), 4.77 (br, 2H), 3.81 (s, 3H); ^{13}C NMR (100.61 MHz, $CDCl_3$) δ = 177.7 (C═O), 159.4 (C), 158.7 (C═N), 138.6 (C), 131.1 (p-CH), 129.2 (2CH), 128.8 (2CH), 128.2 (C), 127.8 (p-CH), 127.7 (2CH), 127.5 (2CH), 122.2 (2CH), 115.3 (2CH), 55.5 (p-OCH_3), 45.2 (N–CH_2). FT-IR (KBr) ν 3376, 3065, 2933, 1652, 1602, 1565, 1510, 1355 e 1205 cm^{-1}. HRESIMS *m/z* 360.1711 $[M+H]^+$ (calcd for $C_{22}H_{22}N_3O_2^+$, 360.1707, Δ = 1.4 ppm). Ret. time 34.83 min, purity 93.7%. m.p. 107.1–107.6 °C.

*4.1.1.9. (Z)–N-((benzylamino) ((4-fluorophenyl)amino)methylene) benzamide (**LQOFG-9**).* Yield 73%. ^{1}H NMR (400.13 MHz, $CDCl_3$) δ = 12.09 (s, 1H), 8.26 (d, *J* = 7.3 Hz, 2H), 7.46 (m, *J* = 7.2 Hz, 1H), 7.40

(m, $J = 7.3$ Hz, 2H), 7.34 (m, 4H), 7.31–7.27 (m, 1H), 7.24 (dd, $J = 8.8$, 2H), 7.09 (t, $J = 8.5$ Hz, 2H), 5.08 (s, 1H), 4.77 (d, $J = 4.6$ Hz, 2H).); ^{13}C NMR (100.61 MHz, $CDCl_3$) $\delta = 177.9$ (C═O), 159.0 (N═C), 138.4 (C), 131.8 (C), 131.3 (p-CH), 129.2 (2CH), 129.1 (2CH), 128.8 (2CH), 127.9 (p-CH), 127.7 (2CH), 127.5 (2CH), 127.0 (2CH), 45.3 (N–CH_2). FT-IR (KBr) ν 3353, 3055, 2931, 1654, 1603, 1566, 1508, 1354 e 1207 cm-1. HRESIMS *m/z* 348.1509 $[M+H]^+$ (calcd for $C_{21}H_{19}FN_3O^+$, 348.1507, $\Delta = -0.8$ ppm). Ret. time 34.97 min, purity 95.1%. m.p. 123.2–123.6 °C.

*4.1.1.10. (Z)–N-((benzylamino) ((4-(trifluoromethyl)phenyl)amino) methylene)benzamide (**LQOFG-10**).* Yield 42%. ^{1}H NMR (400,13 MHz, $CDCl_3$) $\delta = 9.29$ (s, 1H), 9.16 (t, $J = 5.2$ Hz, 1H), 8.12 (d, $J = 8.6$ Hz, 2H), 7.93 (d, $J = 7.2$ Hz, 2H), 7.61 (t, $J = 7.4$ Hz, 1H), 7.52 (d, $J = 7.9$ Hz, 2H), 7.43 (m, 2H), 7.36 (m, 4H), 7.30 (m, 1H), 4.76 (s, 1H), 4.59 (d, $J = 5.9$ Hz, 2H); ^{13}C NMR (100,61 MHz, $CDCl_3$) $\delta = 177.5$ (C═O), 156.5 (C═N), 131.7 (p-CH), 129.1 (2CH), 128.9 (2CH), 128.7(2CH), (2CH + CH), 127.6 (p-CH), 127.5 (2CH), 125.7 (2CH), 57.0 (CF_3), 45.5 (N–CH_2). HRESIMS *m/z* 398.1488 [M+H]+(calcd for $C_{22}H_{18}F_3N_3O^+$, 398.1480, $\Delta = 2.0$ ppm) m.p. dec.

4.2. Biological assays

4.2.1. Parasites

Promastigotes of L. *amazonensis* MPRO/BR/1972/M1841-LV-79 strain was maintained at 28 °C in liver-infusion tryptose medium (LIT) [56] supplemented with 10% heat-inactivated fetal bovine serum (FBS) (Gibco).

4.2.2. Compounds

The guanidine compounds **LQOFG1** – **LQOFG10**, and controls (pentamidine and amphotericin B – AmpB (Sigma-Aldrich)) were dissolved in dimethyl sulfoxide, DMSO, (stock solution, 16.7 mg/mL) and added to the parasite suspension, which furnished ten concentrations ranging from 0.5 to 100 μmol L^{-1} for each compound (final DMSO concentration of 0.1%).

4.2.3. Evaluation of in vitro anti-promastigote activity

In order to determine the half maximal inhibitory concentration (IC_{50}, μM), the MTT colorimetric assay was used as previously described [57,58]. Briefly, *L. amazonensis* promastigote forms were plated in 96-well plates (TPP, Trasadingen, Switzerland) at a density of 1×10^7 parasites/mL (in a final volume of 100 μL) and incubated at 28 °C in the presence of increasing concentrations of guanidine compounds or the reference drugs AmpB or pentamidine for 72 h. Following the incubation period, the MTT assay was done and the formazan crystals were solubilized with a SDS-HCl mix. Then, the absorbance was read at 570 nm (Tecan Infinite M200 PRO, plate reader). The assays were carried out in triplicates and data analysis was determined by nonlinear regression in order to calculate the IC_{50} value.

4.2.4. Evaluation of in vitro activity against L. amazonensis intracellular amastigote

To determine the antileishmanial activity of the guanidine derivatives against intracellular amastigote of *L. amazonensis*, murine peritoneal macrophages obtained as previously described [58] were plated at a density of 3×10^5 cells/well on coverslips (13-mm diameter) previously arranged in a 24-well plate containing RPMI 1640 medium supplemented with 10% inactivated FBS and allowed to adhere for 4 h at 37 °C in 5% CO_2. Adherent macrophages were infected with *Leishmania* promastigotes in the stationary growth phase at a ratio of 5:1 parasite per macrophage at 37 °C in 5% CO_2 for 4 h. The non-internalized parasites were removed by washing and infected cultures were incubated in RPMI 1640 medium for 18 h at 37 °C in 5% CO_2 to allow parasite multiplication. Then, infected cells were treated with different concentrations of compounds, AmpB or pentamidine for 24 h. The cells were fixed with methanol and stained with Giemsa and the number of amastigotes were counted under optical microscopy. The infection index was obtained by multiplying the percentage of infected macrophages by the average number of amastigotes per infected macrophages. The concentration that caused a 50% decrease of growth inhibition compared to the control was also determined by regression analysis and expressed as $IC_{50\text{-ama}}$ in μmol L^{-1}.

4.2.5. Evaluation of cytotoxicity on murine macrophages

Murine macrophages were used for evaluation of compounds cytotoxicity as previously described [58]. Briefly, macrophages were seeded in 96-well flat-bottom plates (TPP, Trasadingen, Switzerland) at a density of 1×10^5 cells/well (100 μL/well) in RPMI 1640 medium supplemented with 10% heat-inactivated FBS, 25 mM HEPES and 2 mM L-glutamine and incubated for 4 h at 37 °C in a 5% CO_2-air mixture, following the addition of the tested compounds or reference drugs at different concentrations. After that, plates were incubated for 24 h at 37 ± 2 °C in a 5% CO_2-air mixture. For the determination of the half-maximal cytotoxic concentrations (CC_{50}, μM), the MTT colorimetric assay was carried out, accordingly to our previous work [57].

4.2.6. Selectivity index

The cytotoxicity for host cells and antiprotozoal activity for promastigotes or intracellular amastigotes forms of *L. amazonensis* were compared as the ratio of the CC_{50}/IC_{50} and expressed as selectivity index (SI).

4.2.7. Anti-leishmanial in vivo evaluation

To evaluate *in vivo* leishmanicidal activity of **LQOFG-2**, female BALB/c mice (20 ± 4 g) 4-weeks-old (CEMIB, UNICAMP) were subcutaneously inoculated at the left hind-footpad with 1×10^7 parasites/mL of infective promastigotes of *L. amazonensis*. Six weeks later, after lesion development, the animals were randomly separated in six groups containing five animals each. The infected animals received daily **LQOFG-2** intraperitoneal doses at 0.13 and 0.25 mg/kg/day for 15 days. Stock solutions of **LQOFG-2** were prepared daily in PBS 1X after solubilization in DMSO (final concentration of 0.1%). A group of mice infected were treated with the reference drug AmpB (2 mg/kg/day – diluted in sterile water according to the manufacturer's instructions) or the vehicle – PBS. Additionally, infected and untreated mice as well as uninfected and untreated mice were also evaluated. Infection was monitored every five days by measuring the thickness of the foot lesions with a dial caliper (Mitutoyo Corp., Japan). Treatment efficacy was determined by the parasite burden of infected feet using limiting dilution methodology [59,60].

4.2.8. Toxicity assay for BALB/c mice

Plasma levels of total bilirubin, aspartate (AST) and alanine (ALT) aminotransferases, alkaline phosphatase (ALP), urea, and creatinine were determined in blood plasma samples collected to BALB/c mice at the end of the treatments, using commercial kits (Labtest Diagnostica S.A., Brazil) [55].

4.2.9. Evaluation of the mutagenicity by micronucleus test in peripheral blood cells of mice

For the evaluation of *in vivo* mutagenicity of compounds peripheral blood cells of male *Mus musculus* (Swiss albino) mice (30 ± 4 g) was used for micronucleus test according to previously described methodology [46]. Briefly, for the treatments, five animals were used per group and each group received 25 mg/kg,

50 mg/kg, and 100 mg/kg of compounds via gavage administered. A positive control group was treated intraperitoneally with cyclophosphamide 50 mg/kg and a negative control group received 0.3 mL of hydroxyethylcellulose 0.5%. Pre-stained laminas by acridine orange (1 mg/mL) were heated at 70 °C and used to analyze the blood collected from the animals. The analysis was performed under a fluorescence microscope, combining blue light (488 nm) and yellow filter. 2000 reticulocytes per animal were counted and recorded the frequencies of micronucleated cells.

4.2.10. Ethics statement

Animal experiments were approved by the Ethics Committee for Animal Experimentation of São Paulo State University (UNESP), School of Pharmaceutical Sciences (CEUA/FCF/CAr n° 33/2016, 44/2016 and 48/2016) in agreement with the guidelines of the Sociedade Brasileira de Ciência de Animais de Laboratorio (SBCAL) and of the Conselho Nacional de Controle da Experimentação Animal (CONCEA).

4.2.11. Statistical analysis

All *in vitro* anti-parasitic assays were carried out in triplicates. The statistical differences between groups were evaluated using the One-way analysis of variance (ANOVA) test followed by Student-Newman-Keuls Multiple Comparisons Test (Graph Pad InStat software) or Tukey test (GraphPad Prism). Differences were considered significant when p-values were ≤ 0.05. For IC_{50} and CC_{50} values, data were processed using the software Origin 7.0 [61].

Declaration of interest

The authors declare no competing financial interest.

Acknowledgements

The authors would like to thank the Brazilian Research Foundations FAPESP (2013/24487-6, 2013/08248-1, 2016/19289-9 and 2017/03552-5), CNPq and CAPES for research fellowships and financial assistance. Authors are thankful to Prof. Chung Man Chin and PhDs Diego Chiba and Daniela Hardman for important help with performance of mutagenicity experiments. We are also grateful to the post-graduation programs of the São Paulo State University (Unesp), “Science and Technology of Materials”, “Pharmaceutical Sciences” and “Biotechnology”, for scientific support.

Appendix A. Supplementary data

Supplementary data to this article can be found online at https://doi.org/10.1016/j.ejmech.2019.03.032.

References

[1] W.H. Organization, Leishmaniasis. https://www.who.int/en/news-room/fact-sheets/detail/leishmaniasis (accessed January 13).
[2] S.L. Croft, S. Sundar, A.H. Fairlamb, Drug resistance in leishmaniasis, Clin. Microbiol. Rev. 19 (1) (2006) 111–126.
[3] S. Natera, C. Machuca, M. Padrón-Nieves, A. Romero, E. Díaz, A. Ponte-Sucre, Leishmania spp.: proficiency of drug-resistant parasites, Int. J. Antimicrob. Agents 29 (6) (2007) 637–642.
[4] S. Croft, P. Olliaro, Leishmaniasis chemotherapy—challenges and opportunities, Clin. Microbiol. Infect. 17 (10) (2011) 1478–1483.
[5] P. Le Pape, Development of new antileishmanial drugs–current knowledge and future prospects, J. Enzym. Inhib. Med. Chem. 23 (5) (2008) 708–718.
[6] J.E. Taylor, S.D. Bull, J.M. Williams, Amidines, isothioureas, and guanidines as nucleophilic catalysts, Chem. Soc. Rev. 41 (6) (2012) 2109–2121.
[7] E.R. Pérez, M.O. da Silva, V.C. Costa, U.P. Rodrigues-Filho, D.W. Franco, Efficient and clean synthesis of N-alkyl carbamates by transcarboxylation and O-alkylation coupled reactions using a DBU–CO2 zwitterionic carbamic complex in aprotic polar media, Tetrahedron Lett. 43 (22) (2002) 4091–4093.
[8] E.R. Pérez, R.H. Santos, M.T. Gambardella, L.G. De Macedo, U.P. Rodrigues-Filho, J.-C. Launay, D.W. Franco, Activation of carbon dioxide by bicyclic amidines, J. Org. Chem. 69 (23) (2004) 8005–8011.
[9] W. McGhee, D. Riley, K. Christ, Y. Pan, B. Parnas, Carbon dioxide as a phosgene replacement: synthesis and mechanistic studies of urethanes from amines, CO_2, and alkyl chlorides, J. Org. Chem. 60 (9) (1995) 2820–2830.
[10] M.A. Casadei, A. Inesi, L. Rossi, Electrochemical activation of carbon dioxide: synthesis of organic carbonates, Tetrahedron Lett. 38 (20) (1997) 3565–3568.
[11] J.M. Hooker, A.T. Reibel, S.M. Hill, M.J. Schueller, J.S. Fowler, One-pot, direct incorporation of [11C] CO2 into carbamates, Angew. Chem. Int. Ed. 48 (19) (2009) 3482–3485.
[12] T. Endo, D. Nagai, T. Monma, H. Yamaguchi, B. Ochiai, A novel construction of a reversible fixation– release system of carbon dioxide by amidines and their polymers, Macromolecules 37 (6) (2004) 2007–2009.
[13] D.J. Darensbourg, R.M. Mackiewicz, Role of the cocatalyst in the copolymerization of CO_2 and cyclohexene oxide utilizing chromium salen complexes, J. Am. Chem. Soc. 127 (40) (2005) 14026–14038.
[14] T. Yamada, P.J. Lukac, M. George, R.G. Weiss, Reversible, room-temperature ionic liquids. Amidinium carbamates derived from amidines and aliphatic primary amines with carbon dioxide, Chem. Mater. 19 (5) (2007) 967–969.
[15] C. Amatore, J.M. Saveant, Mechanism and kinetic characteristics of the electrochemical reduction of carbon dioxide in media of low proton availability, J. Am. Chem. Soc. 103 (17) (1981) 5021–5023.
[16] C. Villiers, J.P. Dognon, R. Pollet, P. Thuéry, M. Ephritikhine, An isolated CO2 adduct of a nitrogen base: crystal and electronic structures, Angew. Chem. 122 (20) (2010) 3543–3546.
[17] J. Ma, X. Zhang, N. Zhao, A.S. Al-Arifi, T. Aouak, Z.A. Al-Othman, F. Xiao, W. Wei, Y. Sun, Theoretical study of TBD-catalyzed carboxylation of propylene glycol with CO2, J. Mol. Catal. A Chem. 315 (1) (2010) 76–81.
[18] T. Mizuno, N. Okamoto, T. Ito, T. Miyata, Synthesis of 2, 4-dihydroxyquinazolines using carbon dioxide in the presence of DBU under mild conditions, Tetrahedron Lett. 41 (7) (2000) 1051–1053.
[19] R.D. do Espírito Santo, R.M. Capitão, E.R.P. González, Guanidines as catalysts for direct and indirect CO_2 capture and activation, in: Guanidines as Reagents and Catalysts II, Springer, 2015, pp. 27–74.
[20] R. D. d. E. Santo, R.C. Simas, A. Magalhães, V. G. d. Santos, T. Regiani, A.C. Isler, N.G. Martins, M.N. Eberlin, E.R.P. González, Experimental NMR and MS study of benzoylguanidines. Investigation of E/Z isomerism, J. Phys. Org. Chem. 26 (4) (2013) 315–321.
[21] L. Qian, H. Xiao, G. Zhao, B. He, Synthesis of modified guanidine-based polymers and their antimicrobial activities revealed by AFM and CLSM, ACS Appl. Mater. Interfaces 3 (6) (2011) 1895–1901.
[22] F. Saczewski, Ł. Balewski, Biological activities of guanidine compounds, Expert Opin. Ther. Pat. 19 (10) (2009) 1417–1448.
[23] H.-m. Hua, J. Peng, F.R. Fronczek, M. Kelly, M.T. Hamann, Crystallographic and NMR studies of antiinfective tricyclic guanidine alkaloids from the sponge Monanchora unguifera, Bioorg. Med. Chem. 12 (24) (2004) 6461–6464.
[24] J.H. Short, C.W. Ours, W.J. Ranus Jr., Sympathetic nervous system blocking agents. V. Derivatives of isobutyl-, tert-butyl-, and neopentylguanidine, J. Med. Chem. 11 (6) (1968) 1129–1135.
[25] T. Satoh, M. Muramatu, Y. Ooi, H. Miyataka, T. Nakajima, M. Umeyama, Medicinal chemical studies on synthetic protease inhibitors, trans-4-guanidinomethylcyclohexanecarboxylic acid aryl esters, Chem. Pharm. Bull. 33 (2) (1985) 647–654.
[26] Y. Miyamoto, H. Hirose, H. Matsuda, S. Nakano, M. Ohtani, M. Kaneko, K. Nishigaki, F. Nomura, H. Kitamura, Y. Kawashima, Analysis of complement activation profile during cardiopulmonary bypass and its inhibition by fut–175, Am. Soc. Artif. Intern. Organs J. 31 (1) (1985) 508–511.
[27] K. Okumura, Y. Kiyohara, F. Komada, S. Iwakawa, M. Hirai, T. Fuwa, Improvement in wound healing by epidermal growth factor (EGF) ointment. I. Effect of nafamostat, gabexate, or gelatin on stabilization and efficacy of EGF, Pharmaceut. Res. 7 (12) (1990) 1289–1293.
[28] I. Muramatsu, M. Oshita, K. Yamanaka, Selective alpha-2 blocking action of DG-5128 in the dog mesenteric artery and rat vas deferens, J. Pharmacol. Exp. Ther. 227 (1) (1983) 194–198.
[29] S. Umezawa, Y. Takahashi, T. Usui, T. Tsuchiya, Total synthesis of streptomycin, J. Antibiot. 27 (12) (1974) 997–999.
[30] S. Marriner, Anthelmintic drugs, Vet. Rec. 118 (7) (1986) 181–184.
[31] C.E. Stephens, R. Brun, M.M. Salem, K.A. Werbovetz, F. Tanious, W.D. Wilson, D.W. Boykin, The activity of diguanidino and ‘reversed’diamidino 2, 5-diarylfurans versus Trypanosoma cruzi and Leishmania donovani, Bioorg. Med. Chem. Lett 13 (12) (2003) 2065–2069.
[32] P. Bilbao-Ramos, C. Galiana-Roselló, M.A. Dea-Ayuela, M. González-Alvarez, C. Vega, M. Rolón, J. Pérez-Serrano, F. Bolás-Fernández, M.E. González-Rosende, Nuclease activity and ultrastructural effects of new sulfonamides with anti-leishmanial and trypanocidal activities, Parasitol. Int. 61 (4) (2012) 604–613.
[33] L.F. Martins, J.T. Mesquita, E.G. Pinto, T.A. Costa-Silva, S.E. Borborema, A.J. Galisteo Junior, B.J. Neves, C.H. Andrade, Z.A. Shuhaib, E.L. Bennett, Analogues of marine guanidine alkaloids are in vitro effective against Trypanosoma cruzi and selectively eliminate Leishmania (L.) infantum Intracellular amastigotes, J. Nat. Prod. 79 (9) (2016) 2202–2210.
[34] B. Freedlander, F.A. French, Carcinostatic action of polycarbonyl compounds and their derivatives: II. Glyoxal bis (Guanylhydrazone) and derivatives, Cancer Res. 18 (3) (1958) 360–363.
[35] J.V. Greenhill, P. Lue, 5 amidines and guanidines in medicinal chemistry, in:

Progress in Medicinal Chemistry, vol. 30, Elsevier, 1993, pp. 203–326.
[36] R.G. Berlinck, M.H. Kossuga, Natural guanidine derivatives, Nat. Prod. Rep. 22 (4) (2005) 516–550.
[37] D.J. Faulkner, Highlights of marine natural products chemistry (1972–1999), Nat. Prod. Rep. 17 (1) (2000) 1–6.
[38] D. do Espirito Santo, R, G.M. Machado, M, L. dos Santos, J, R.P. Gonzalez, E, M. Chin, C, Use of guanidine compounds in the treatment of neglected tropical diseases, Curr. Org. Chem. 18 (20) (2014) 2572–2602.
[39] E.V. Costa, M.L.B. Pinheiro, C.M. Xavier, J.R. Silva, A.C.F. Amaral, A.D. Souza, A. Barison, F.R. Campos, A.G. Ferreira, G.M. Machado, A pyrimidine-β-carboline and other alkaloids from annona f oetida with antileishmanial activity, J. Nat. Prod. 69 (2) (2006) 292–294.
[40] K. Agarwal, V. Sharma, N. Shakya, S. Gupta, Design and synthesis of novel substituted quinazoline derivatives as antileishmanial agents, Bioorg. Med. Chem. Lett 19 (18) (2009) 5474–5477.
[41] M.A. Dea-Ayuela, E. Castillo, M. Gonzalez-Alvarez, C. Vega, M. Rolón, F. Bolás-Fernández, J. Borrás, M.E. González-Rosende, In vivo and in vitro antileishmanial activities of 4-nitro-N-pyrimidin-and N-pyrazin-2-ylbenzenesulfonamides, and N2-(4-nitrophenyl)-N1-propylglycinamide, Bioorg. Med. Chem. 17 (21) (2009) 7449–7456.
[42] M.A. Giulianotti, B.A. Vesely, A. Azhari, A. Souza, T. LaVoi, R.A. Houghten, D.E. Kyle, J.W. Leahy, Identification of a hit series of antileishmanial compounds through the use of mixture-based libraries, ACS Med. Chem. Lett. 8 (8) (2017) 802–807.
[43] Q.-J. Li, C.-L. Yang, Synthesis and crystal structure of a compound with two conformational isomers: N-(2-methylbenzoyl)-N′-(4-nitrophenyl) thiourea, J. Chem. Crystallogr. 38 (12) (2008) 927–930.
[44] R. D. d. Espírito Santo, Síntese, caracterização e estudo do isomerismo E/Z de benzoilguanidinas, 2013.
[45] S. Cunha, B.R. de Lima, A.R. de Souza, Bismuth nitrate pentahydrate: a new and environmentally benign reagent for guanidylation of N-benzoylthioureas, Tetrahedron Lett. 43 (1) (2002) 49–52.
[46] J.L. Santos, P.L. Bosquesi, A.E. Almeida, C.M. Chin, E.A. Varanda, Mutagenic and genotoxic effect of hydroxyurea, Int. J. Biomed. Sci.: IJBS 7 (4) (2011) 263.
[47] M. Hayashi, The micronucleus test—most widely used in vivo genotoxicity test—, Genes Environ. 38 (1) (2016) 18.
[48] M.F. Santos, P.M. Harper, D.E. Williams, J.T. Mesquita, E.G. Pinto, T.A. da Costa-Silva, E. Hajdu, A.G. Ferreira, R.A. Santos, P.J. Murphy, Anti-parasitic guanidine and pyrimidine alkaloids from the marine sponge Monanchora arbuscula, J. Nat. Prod. 78 (5) (2015) 1101–1112.
[49] K.H. Barrosa, E.G. Pinto, A.G. Tempone, E.G.A. Martins, J.H.G. Lago, Alchornedine, a new anti-trypanosomal guanidine alkaloid from Alchornea glandulosa, Planta Med. 80 (15) (2014) 1310–1314.
[50] N. Ahmed, K.G. Brahmbhatt, S.I. Khan, M. Jacob, B.L. Tekwani, S. Sabde, D. Mitra, I.P. Singh, I.A. Khan, K.K. Bhutani, Synthesis and biological evaluation of tricyclic guanidine analogues of batzelladine K for antimalarial, antileishmanial, antibacterial, antifungal, and anti-HIV activities, Chem. Biol. Drug Des. 81 (4) (2013) 491–498.
[51] J.L. Gonzalez, C.E. Stephens, T. Wenzler, R. Brun, F.A. Tanious, W.D. Wilson, T. Barszcz, K.A. Werbovetz, D.W. Boykin, Synthesis and antiparasitic evaluation of bis-2, 5-[4-guanidinophenyl] thiophenes, Eur. J. Med. Chem. 42 (4) (2007) 552–557.
[52] C. Kratzer, S. Tobudic, K. Macfelda, W. Graninger, A. Georgopoulos, In vivo activity of a novel polymeric guanidine in experimental skin infection with methicillin-resistant Staphylococcus aureus, Antimicrob. Agents Chemother. 51 (9) (2007) 3437–3439.
[53] R.K. Arafa, R. Brun, T. Wenzler, F.A. Tanious, W.D. Wilson, C.E. Stephens, D.W. Boykin, Synthesis, DNA affinity, and antiprotozoal activity of fused ring dicationic compounds and their prodrugs, J. Med. Chem. 48 (17) (2005) 5480–5488.
[54] K. Katsuno, J.N. Burrows, K. Duncan, R.H. Van Huijsduijnen, T. Kaneko, K. Kita, C.E. Mowbray, D. Schmatz, P. Warner, B. Slingsby, Hit and lead criteria in drug discovery for infectious diseases of the developing world, Nat. Rev. Drug Discov. 14 (11) (2015) 751.
[55] A.M.A. Velásquez, W.C. Ribeiro, V. Venn, S. Castelli, M. S. d. Camargo, R.P. de Assis, R.A. de Souza, A.R. Ribeiro, T.G. Passalacqua, J.A. da Rosa, A.M. Baviera, A.E. Mauro, A. Desideri, E.E. Almeida-Amaral, M.A.S. Graminha, Efficacy of a binuclear cyclopalladated compound therapy for cutaneous leishmaniasis in the murine model of infection with *Leishmania amazonensis* and its inhibitory effect on Topoisomerase 1B, Antimicrob. Agents Chemother. 61 (8) (2017) e00688-17.
[56] L. d. Silva, Sobre uma cepa de Trypanosoma cruzi altamente virulenta para o camundongo branco, Folia Clin. Biol. 20 (1953) 191–207.
[57] A. Velásquez, R. A. d. Souza, T.G. Passalacqua, A.R. Ribeiro, M. Scontri, C.M. Chin, L. d. Almeida, M.L.D. Cistia, J. A. d. Rosa, A.E. Mauro, Antiprotozoal activity of the cyclopalladated complexes against Leishmania amazonensis and Trypanosoma cruzi, J. Braz. Chem. Soc. 27 (6) (2016) 1032–1039.
[58] T.G. Passalacqua, L.A. Dutra, L. de Almeida, A.M.A. Velásquez, F.A.E. Torres, P.R. Yamasaki, M.B. dos Santos, L.O. Regasini, P.A. Michels, V. da Silva Bolzani, Synthesis and evaluation of novel prenylated chalcone derivatives as antileishmanial and anti-trypanosomal compounds, Bioorg. Med. Chem. Lett 25 (16) (2015) 3342–3345.
[59] H.C. Lima, J.A. Bleyenberg, R.G. Titus, A simple method for quantifying Leishmania in tissues of infected animals, Parasitol. Today 13 (2) (1997) 80–82.
[60] L. de Almeida, T.G. Passalacqua, L.A. Dutra, J. N. V. d. Fonseca, R.F.Q. Nascimento, K.B. Imamura, C.R. de Andrade, J.L. dos Santos, M.A.S. Graminha, In vivo antileishmanial activity and histopathological evaluation in Leishmania infantum infected hamsters after treatment with a furoxan derivative, Biomed. Pharmacother. 95 (2017) 536–547.
[61] P.M. Edwards, Origin 7.0: scientific graphing and data analysis software, J. Chem. Inf. Comput. Sci. 42 (5) (2002) 1270–1271.